Electronic Supplementary Material (ESI) for Journal of Materials Chemistry A.

Supporting Information

Bimetallic $Co_2Mo_3O_8$ suboxides coupled with conductive cobalt nanowires for efficient and durable hydrogen evolution in alkaline electrolyte

Yingqing Ou[a], Weiquan Tian[a], Lu Liu[c], Yunhuai Zhang[a] and Peng Xiao[b*]*

[a]*College of Chemistry and Chemical Engineering, Chongqing University, Chongqing 401331, China*

[b]*College of Physics, Chongqing University, Chongqing 401331, China*

[c]*College of Materials Science and Engineering, Chongqing University, Chongqing 400044, China*

AUTHOR INFORMATION

Corresponding Authors

*Tel. +86 13883077781; +86 15823038874.

To whom correspondence should be addressed:

(Y. H. Zhang) xp2031@163.com;

(P. Xiao) xiaopeng@cqu.edu.cn

Notes

The authors declare no competing financial interest.

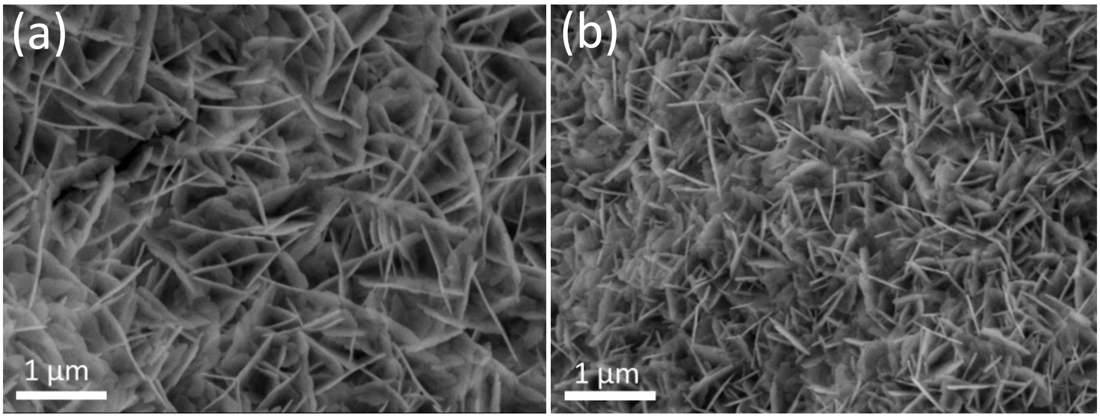

Fig. S1 SEM images of (a) $CoMoO_4 \cdot 0.9H_2O$/NF and (b) $Co_2Mo_3O_8$/NF

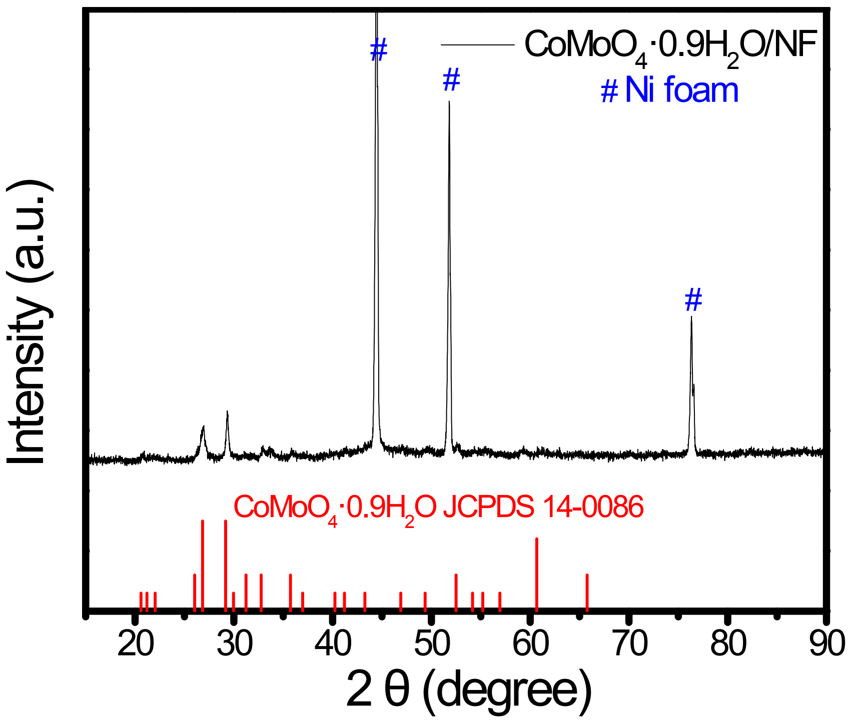

Fig. S2 XRD pattern of $CoMoO_4 \cdot 0.9H_2O$ supported on Ni foam.

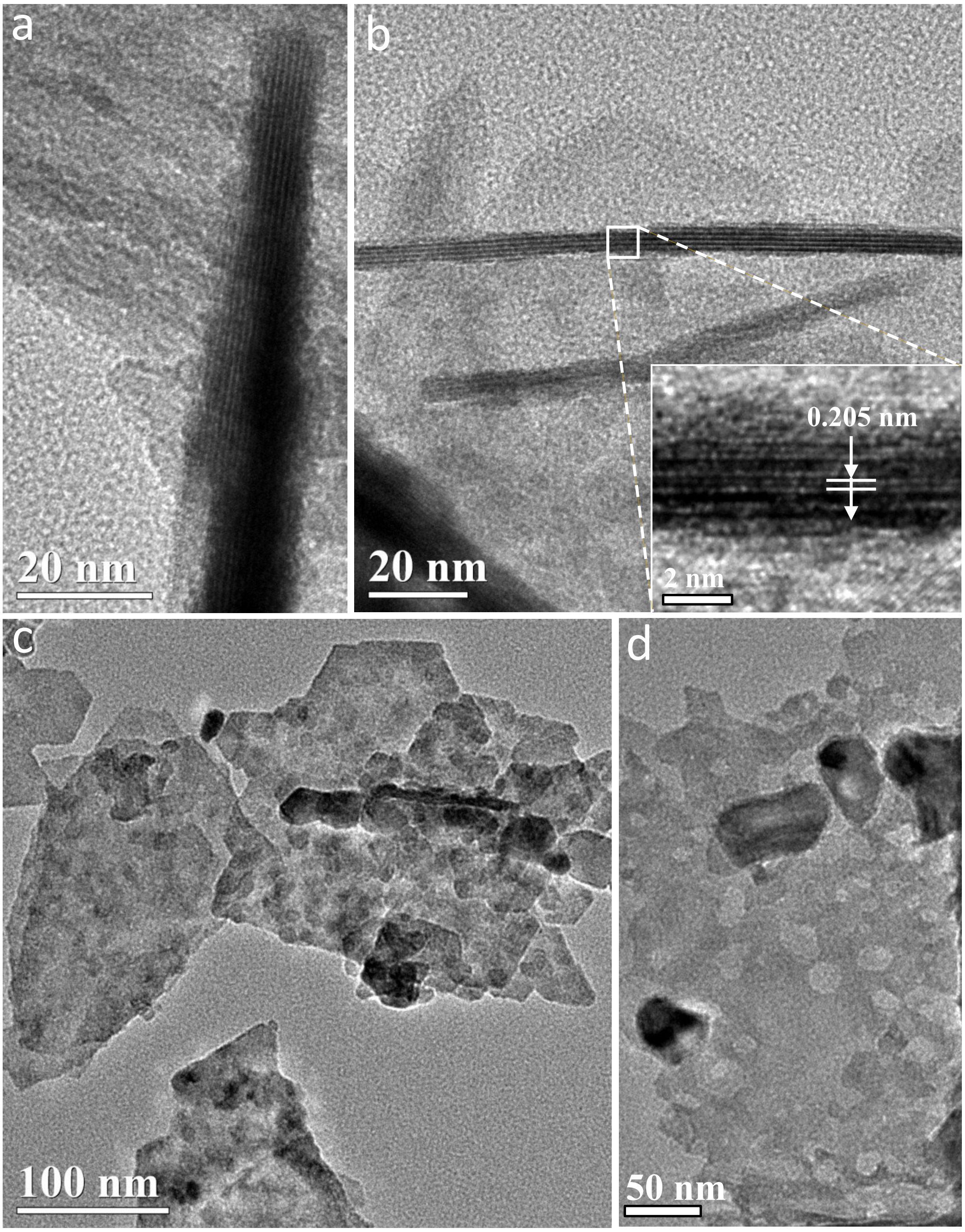

Fig. S3 (a,b) TEM images of the tip region of Co nanowires. The inset in b shows the lattice fringe of the Co nanowire. (c,d) TEM images of $Co_2Mo_3O_8$ nanosheets with tiny pores (20~40 nm).

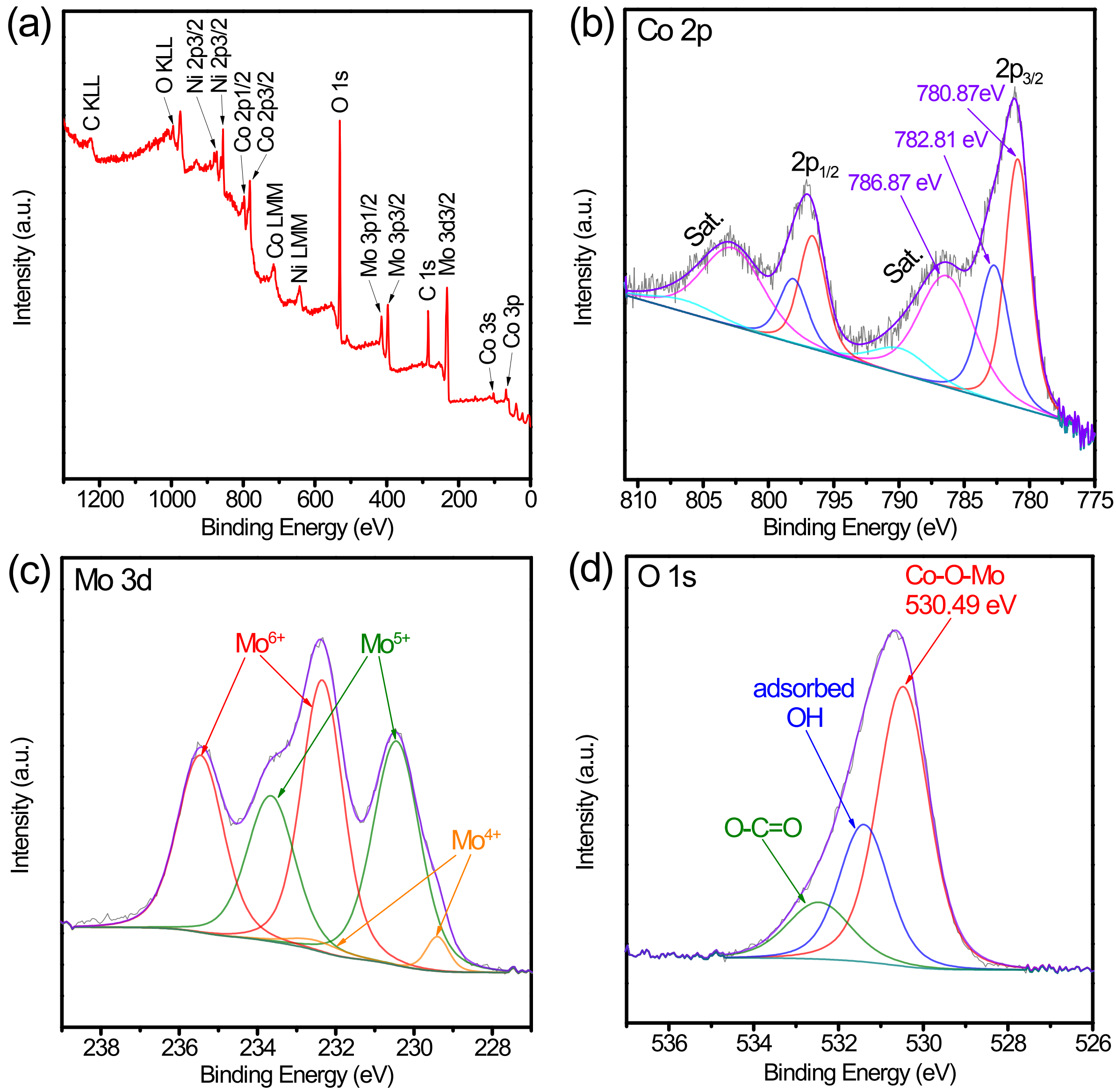

Fig. S4 (a) XPS survey spectrum of $Co_2Mo_3O_8$/NF. High-resolution XPS spectrum of (b) Co 2p region, (c) Mo 3d region, and (d) O 1s region of $Co_2Mo_3O_8$/NF.

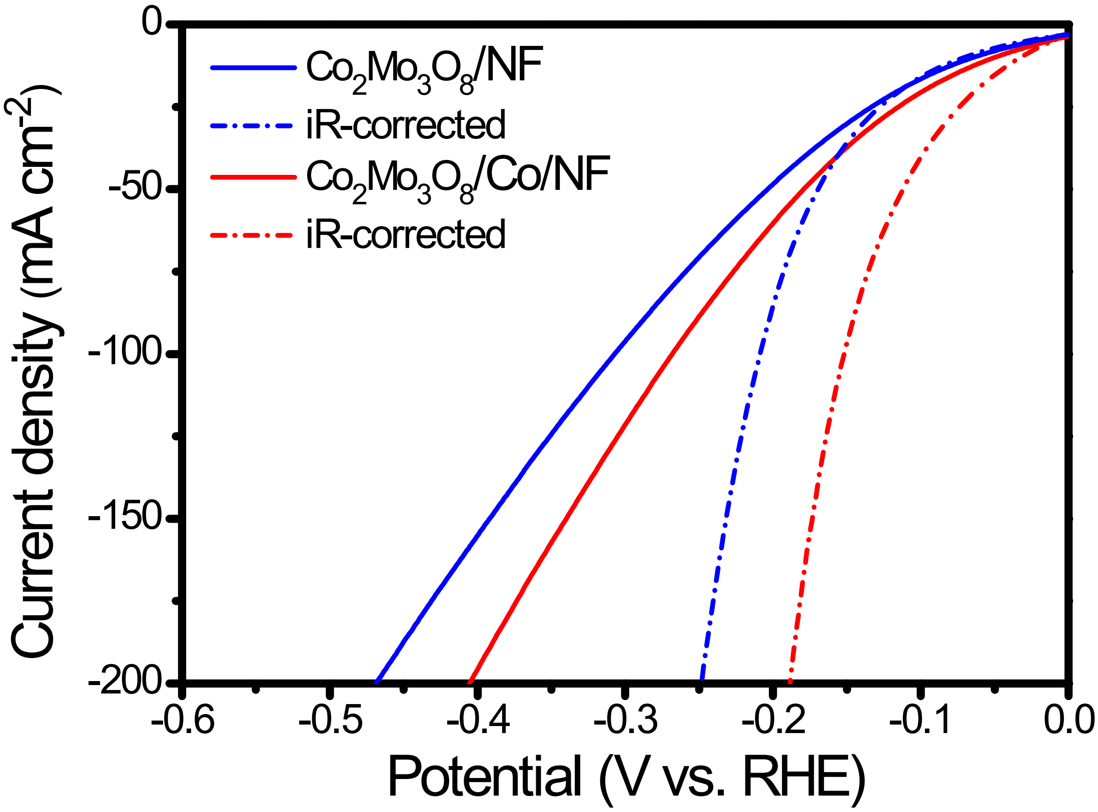

Fig. S5 Polarization curves of $Co_2Mo_3O_8$/NF and $Co_2Mo_3O_8$/Co/NF before and after iR-compensation (90%) in 1.0 M KOH.

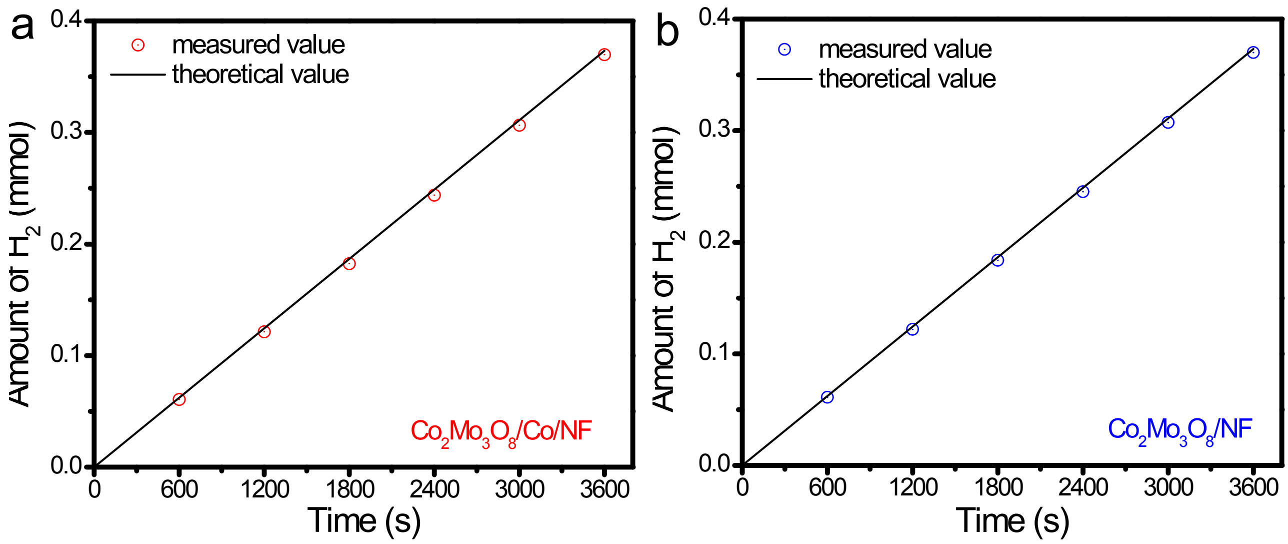

Fig. S6 The amount of experimentally measured and theoretically calculated H_2 versus time for (a) $Co_2Mo_3O_8$/Co/NF and (b) $Co_2Mo_3O_8$/NF. A constant current of 10 mA was applied for 3,600 s; the electrolyte was 1.0 M KOH.

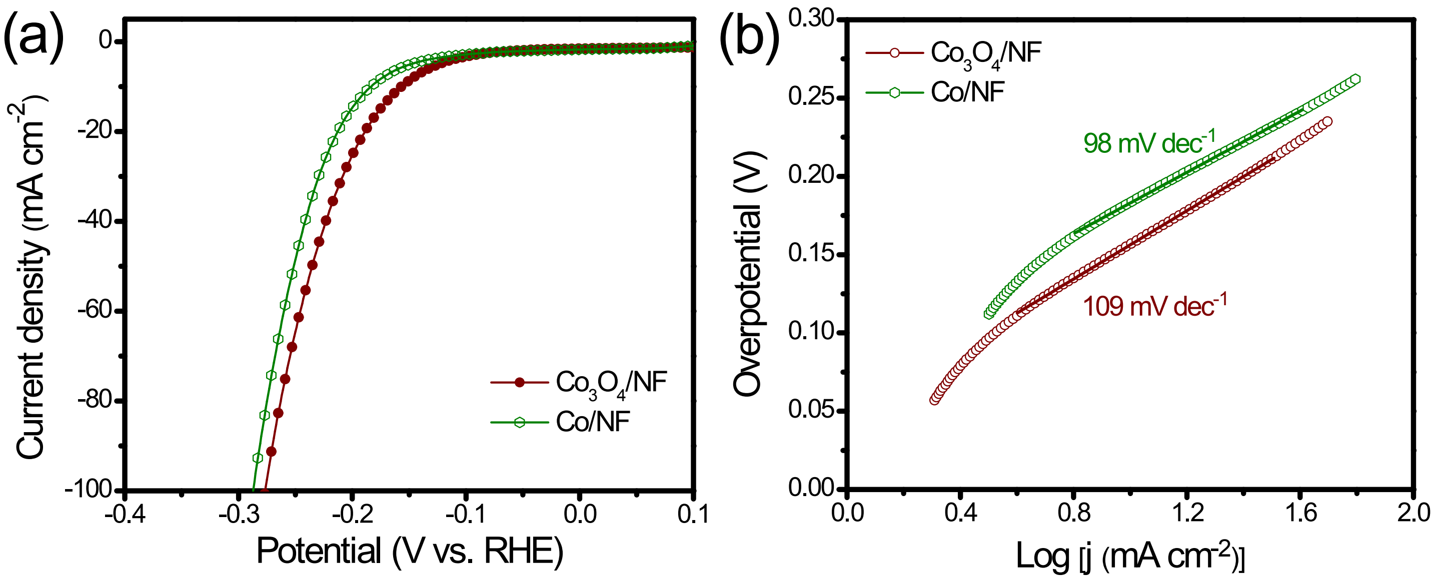

Fig. S7 (a) LSV curves of Co_3O_4/NF and Co/NF at a scan rate of 1 mV s^{-1} in 1.0 M KOH (with 90 iR-compensation) . (b) Tafel plots derived from the LSV curves of the electrocatalysts. The HER activity of Co_3O_4 and Co nanowires supported on Ni foam was investigated as well. The Co_3O_4/NF and Co/NF yield a current density of 10 mA cm^{-2} at overpotentials of 164 mV and 191 mV, respectively, much higher than the $Co_2Mo_3O_8$-based electrodes. Meanwhile, the Tafel slopes of Co_3O_4/NF (109 mV dec^{-1}) and Co/NF (98 mV dec^{-1}) are also higher than the $Co_2Mo_3O_8$-based electrodes. The above results verify the important role of $Co_2Mo_3O_8$ in the efficient hydrogen evolution.

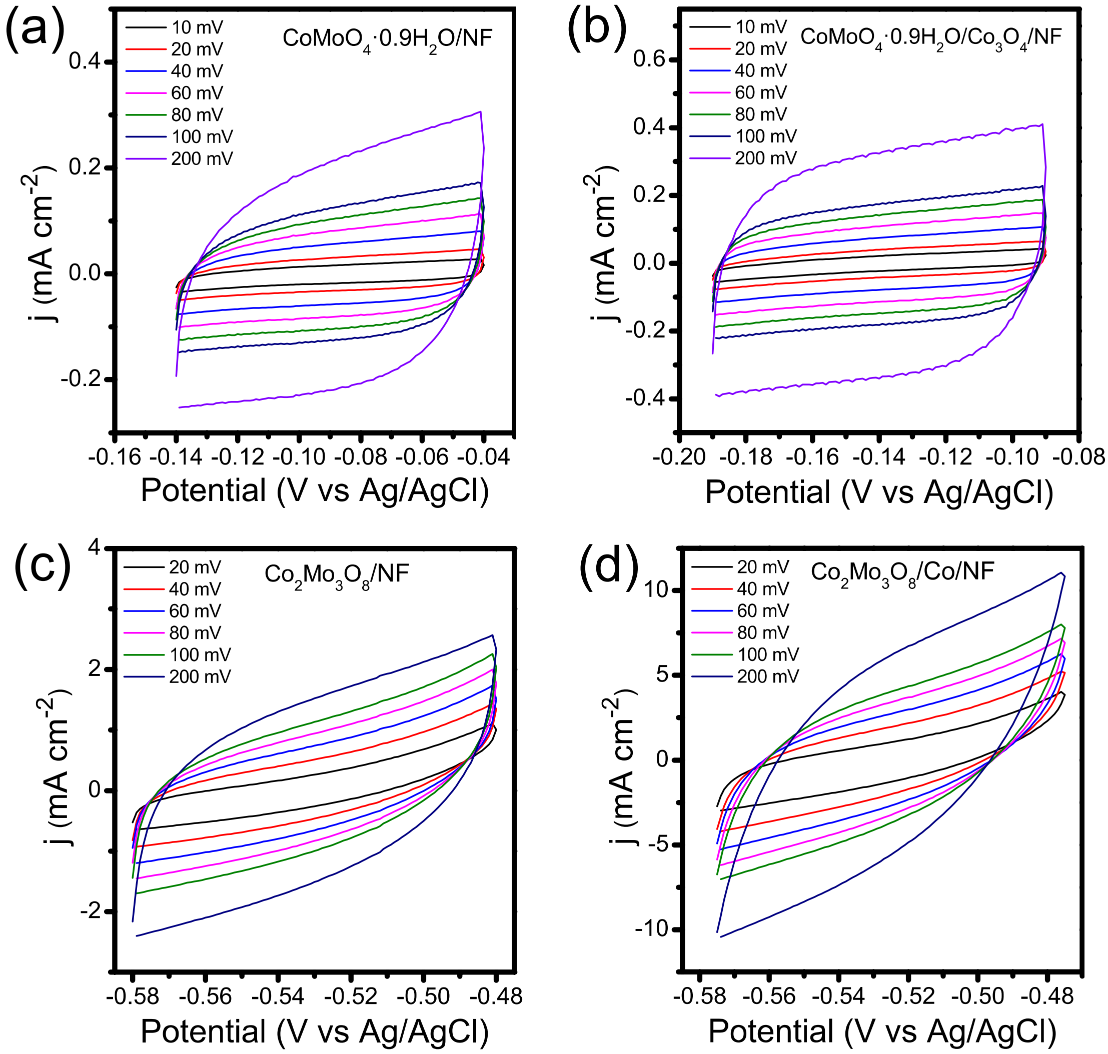

Fig. S8 Cyclic voltammetry (CV) tests at different scan rates in non-Faradaic regions for (a) $CoMoO_4 \cdot 0.9H_2O$/NF, (b) $CoMoO_4 \cdot 0.9H_2O/Co_3O_4$/NF, (c) $Co_2Mo_3O_8$/NF and (d) $Co_2Mo_3O_8$/Co/NF electrodes.

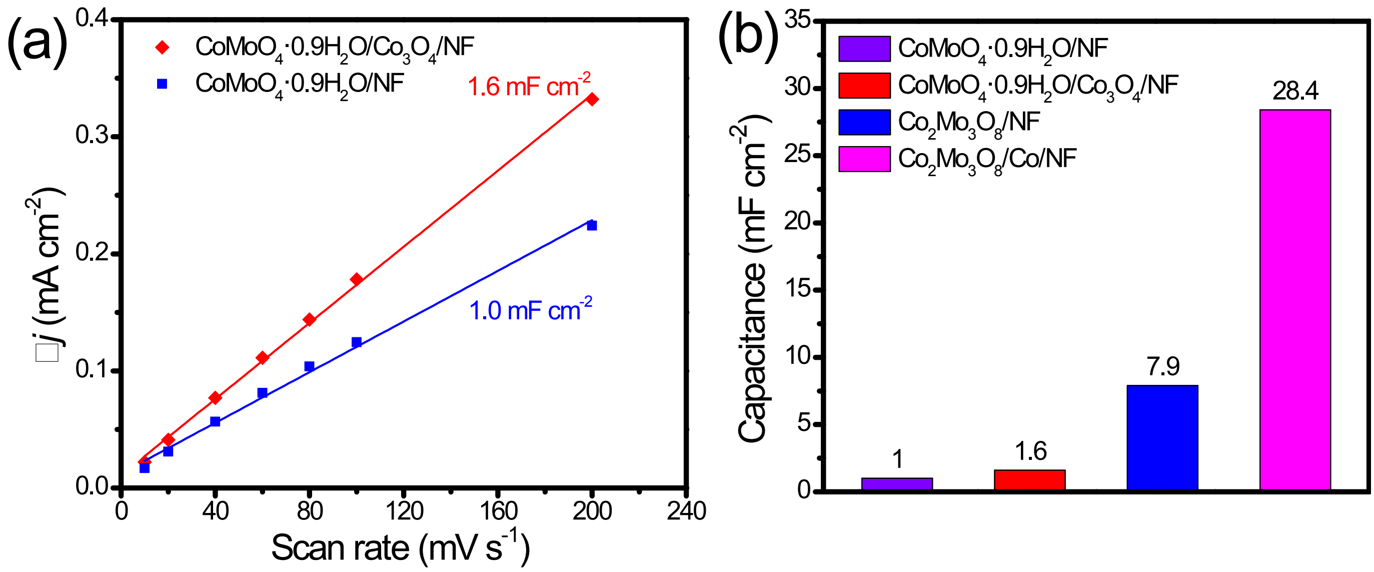

Fig. S9 (a) The current density variation ($\Delta j = (j_a - j_c)/2$, at -0.09 V *vs* Ag/AgCl for $CoMoO_4{\cdot}0.9H_2O$/NF and -0.14 V *vs* Ag/AgCl for $CoMoO_4{\cdot}0.9H_2O/Co_3O_4$/NF) against the scan rates of Cyclic Voltammetry (CV) measurements. The Δj as a function of the scan rate yields a straight line and the slope of this straight line is equal to the value of C_{DL}. (b) Comparison of the calculated electrochemical double layer capacitance (C_{DL}) of different electrocatalysts in this work.

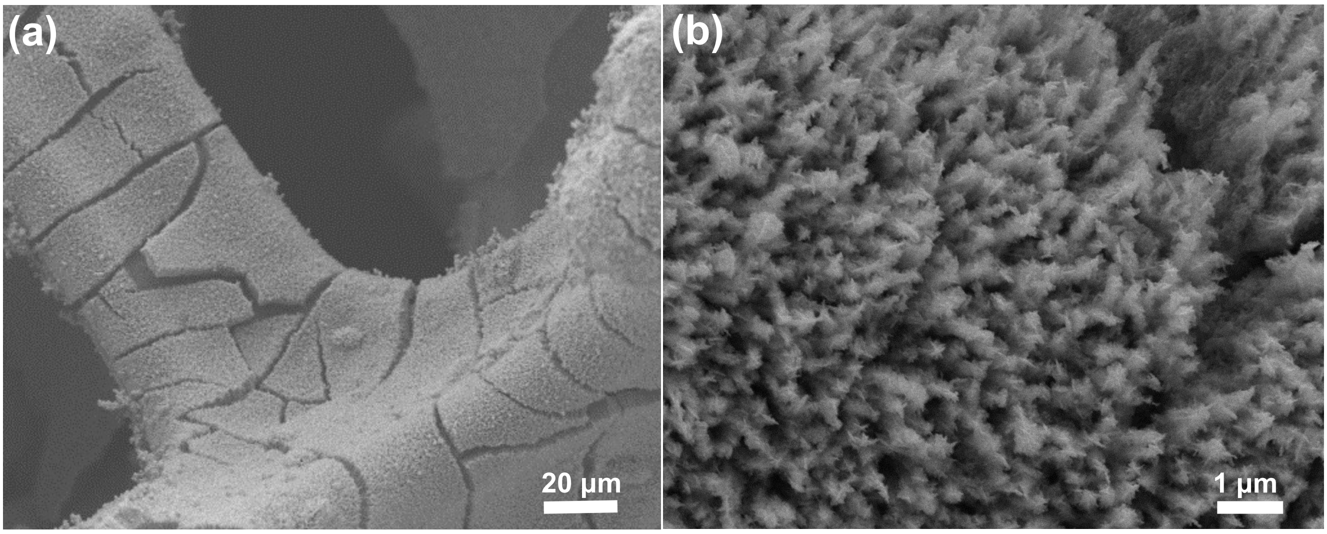

Fig. S10 (a,b) SEM images of $Co_2Mo_3O_8$/Co/NF after stability test at different magnifications.

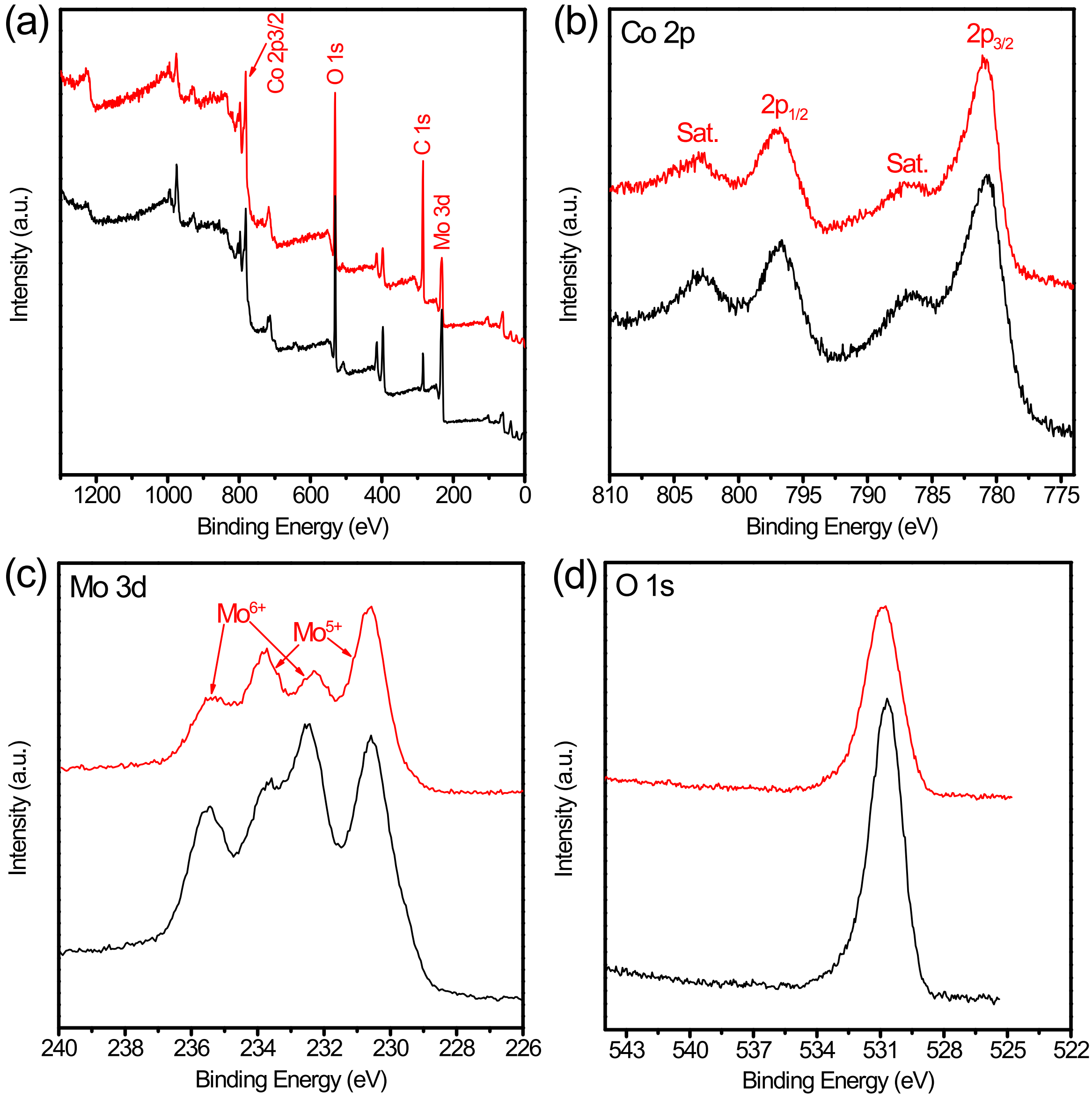

Fig. S11XPS spectra of $Co_2Mo_3O_8$/Co/NF electrocatalyst before (black) and after 20 h chronopotentiometry test (red). (a) XPS survey spectra, and high-resolution XPS spectra of (b) Co 2p region, (c) Mo 3d region and (d) O 1s region.

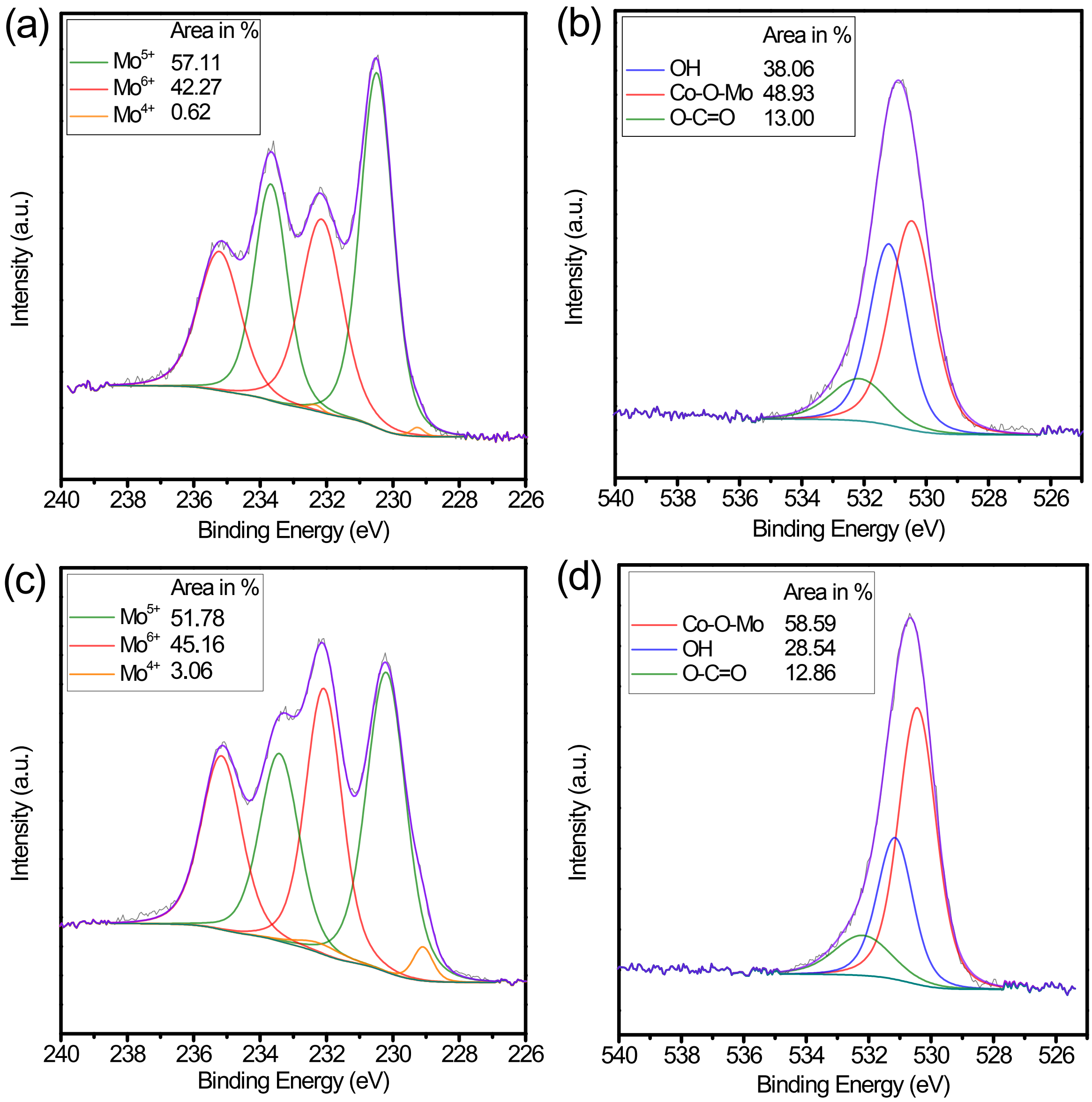

Fig. S12 Curve-fitted high-resolution XPS spectra of (a) Mo 3d region, (b) O 1s region of the $Co_2Mo_3O_8$/Co/NF electrocatalyst after 20 h chronopotentiometry test, (c) Mo 3d region and (d) O 1s region of the as-prepared $Co_2Mo_3O_8$/Co/NF.

Table S1. The HER catalytic activities of $Co_2Mo_3O_8$-based eletrocatalysts in this work and reported non-noble metal electrocatalysts in alkaline solutions.

Electrocatalysts	Onset overpotential (mv)	Overpotential (mV) at 10 mA cm^{-2}	Tafel slope (mV dec^{-1})	Electrolyte	Ref.
$Co_2Mo_3O_8$/Co/NF	9	50	49	1.0 M KOH	This work
$Co_2Mo_3O_8$/NF	16	85	88	1.0 M KOH	This work
Co-Mo nanoparticles	—	75	—	1.0 M KOH	[1]
Co-Mo_2C nanowires	25	118	44	1.0 M KOH	[2]
Mesoporous MoO_{3-x}	—	138	56	0.1 M KOH	[3]
Nanoflower-like MoO_2/NF	~0	55	66	1.0 M KOH	[4]
N,P-Doped Mo_2C@C nanospheres	—	47	71	1.0 M KOH	[5]
S and N codoped MoP	—	49	31	1.0 M KOH	[6]
Mo_2C nanoparticels on carbon microflowers	38	100	65	1.0 M KOH	[7]
Co/Co_3O_4 core/shell nanosheets	~30	129 mV at 20 mA cm^{-2}	44	1.0 M KOH	[8]
Hollow Co_3O_4 microtube arrays	100	190 mV at 20 mA cm^{-2}	98	1.0 M KOH	[9]
$Co(OH)_2$@PANI hybrid nanosheets	50	90	92	1.0 M KOH	[10]
Ni-Mo nanopowders	—	70 mV at 20 mA cm^{-2}	—	2.0 M KOH	[11]
NiMo alloy nanowires	—	30	86	1.0 M KOH	[12]
Ni_2P/Ni/NF	40	98	72	1.0 M KOH	[13]
CoP/CC	115	209	129	1.0 M KOH	[14]
FeP NAs/CC	86	218	146	1.0 M KOH	[15]
c-$CoSe_2$/CC	—	190	85	1.0 M KOH	[16]
NiSe/NF	—	96	120	1.0 M KOH	[17]
$NiCo_2S_4$ NW/NF	—	210	58.9	1.0 M KOH	[18]

$NiCo_2S_4$/NF	17	65	84.5	1.0 M KOH	[19]
NiFe LDH/$NiCo_2O_4$/NF	83	192	59	1.0 M KOH	[20]
NiCoFe LTHs/CFC	180	200	70	1.0 M KOH	[21]

References

[1] J. M. McEnaney, T. L. Soucy, J. M. Hodges, J. F. Callejas, J. S. Mondschein, R. E. Schaak, *J. Mater. Chem. A* **2016**, *4*, 3077.

[2] H. Lin, N. Liu, Z. Shi, Y. Guo, Y. Tang, Q, Gao, *Adv. Funct. Mater*. **2016**, *26*, 5590.

[3] Z. Luo, R. Miao, T. D. Huan, I. M. Mosa, A. S. Poyraz, W. Zhong, J. E. Cloud, D. A. Kriz, S. Thanneeru, J. He, Y. Zhang, R. Ramprasad, S. L. Suib, *Adv. Energy Mater*. **2016**, *6*, 1600528.

[4] Y. Jin, P. K. Shen, *J. Mater. Chem. A* **2015**, *3*, 20080.

[5] Y. Chen, Y. Zhang, W. Jiang, X. Zhang, Z. Dai, L. Wan, J. Hu, *ACS Nano* **2016**, *10*, 8851.

[6] M. A. R. Anjum, J. S. Lee, *ACS Catal*. **2017**, *7*, 3030.

[7] Y. Huang, Q. Gong, X. Song, K. Feng, K. Nie, F. Zhao, Y. Wang, M. Zeng, J. Zhong, Y. Li, *ACS Nano* **2016**,*10*, 11337.

[8] X. Yan, L. Tian, M. He, X. Chen, *Nano Lett*. **2015**, *15*, 6015.

[9] Y. Zhu, T. Ma, M. Jaroniec, S. Qiao, *Angew. Chem. Int. Ed*. **2016**, *55*, 1.

[10] J. Feng, L. Ding, S. Ye, X. He, H. Xu, Y. Tong, G. Li, *Adv. Mater*. **2015**, *27*, 7051.

[11] J. R. McKone, B. F. Sadtler, C. A. Werlang, N. S. Lewis, H. B. Gray, *ACS Catal*.

2013, *3*, 166.

[12] M. Fang, W. Gao, G. Dong, Z. Xia, S. Yip, Y. Qin, Y. Qu, J. C. Ho, *Nano Energy* **2016**, *27*, 147.

[13] B. You, N. Jiang, M. Sheng, M. W. Bhushan, Y. Sun, *ACS Catal*. **2016**, *6*, 714.

[14] J. Tian, Q. Liu, A. M. Asiri, X. Sun, *J. Am. Chem. Soc*. **2014**, *136*, 7587.

[15] Y. Liang, Q. Liu, A. M. Asiri, X. Sun, Y. Luo, *ACS Catal*. **2014**, *4*, 4065.

[16] P. Chen, K. Xu, S. Tao, T. Zhou, Y. Tong, H. Ding, L. Zhang, W. Chu, C. Wu, Y. Xie, *Adv. Mater*. **2016**, *28*, 7527.

[17] C. Tang, N. Cheng, Z. Pu, W. Xing, X. Sun, *Angew. Chem*. **2015**, *127*, 9483.

[18] A. Sivanantham, P. Ganesan, S. Shanmugam, *Adv. Funct. Mater*. **2016**, *26*, 4661.

[19] L. Ma, Y. Hu, R. Chen, G. Zhu, T. Chen, H. Lv, Y. Wang, J. Liang, H. Liu, C. Yan, H. Zhu, Z. Tie, Z. Jin, J. Liu, *Nano Energy* **2016**, *24*, 139.

[20] Z. Wang, S. Zeng, W. Liu, X. Wang, Q. Li, Z. Zhao, F. Geng, *ACS Appl. Mater. Interfaces*. **2017**, *9*, 1488.

[21] A. Wang, H. Xu, G. Li, *ACS Energy Lett*. **2016**, *1*, 445.